

Identification of Oscillatory Modes in Power System Responses via Vector Fitting

T. A. Papadopoulos, A. I. Chrysochos, E. O. Kontis, G. K. Papagiannis

Abstract—System identification methods have been widely used for the study of low frequency electromechanical oscillations and the development of low order dynamic models. This paper introduces vector fitting (VF) to estimate the eigenvalues of power systems based on their dynamic responses. Practical issues and solutions encountered in the application of VF are discussed. The performance of VF is evaluated in different power system models and is found very accurate in all cases.

Keywords: mode estimation, rational approximation, ringdown analysis, oscillation modes, system identification, vector fitting.

I. INTRODUCTION

DYNAMIC or small-signal stability studies are of crucial importance for the planning, control and safe operation of power systems. In order to analyze power system dynamics, linear analysis or system identification techniques are used [1].

Linear analysis is a standard tool in most simulation platforms, which requires the determination of a detailed model to be analyzed using eigenanalysis and control methods. On the other hand, system identification techniques are advanced mathematical tools that directly reflect the dominant dynamic characteristics of a system using data sets, comprising either offline simulated data or online measurements. System identification consists of three main steps: a) the design of an experiment, b) the implementation of a system model, and c) the estimation of the model parameters from measurements.

Significant applications of the system identification approach include: a) tuning, design and testing of control systems, b) control signal analysis, c) model validation to verify and improve the accuracy of linear models as well as of the used data for parameters, and d) incorporation of robust control design techniques [2]. Moreover, system identification also deals with the development of low order equivalent models for the analysis of the dynamic performance of power systems, following either the black- or the grey-box approach. Dynamic equivalencing is an approach to overcome the

difficulties of detailed modeling, especially in complex distribution networks, due to the efficient computational performance and the ability to model different types of energy sources and loads.

Several system identification techniques have been proposed in the literature. The majority of them are based on the direct identification of the model parameters from time-domain (TD) responses, including the Prony method [3], the numerical algorithm for sub-space state space system identification (N4SID) [4], and the prediction error method (PEM) [5]. However, system modes were originally estimated in frequency-domain (FD) from the spectrum of a dynamic response, by applying the fast Fourier transform (FFT) [6], combined also with the sliding window technique for the damping factor estimation. In 1999, a powerful and very accurate method for system identification in the frequency domain was proposed, known as vector fitting (VF) [7]. The basic concept of VF is that it utilizes rational approximations in order to estimate the zeros and poles of a FD function. Since then, VF has been widely applied to a number of power system problems, including the modeling of transmission lines, power transformers, high-speed interconnects, etc. The significant advantage of VF is that it provides very accurate fitting with guaranteed stable poles, which can be also applied to multiterminal systems [8].

In this paper, the VF technique is adopted for the first time to identify the oscillatory modes contained in dynamic responses of power systems, when the system is subjected to small disturbances. The procedure is implemented in two steps: 1) the dynamic responses are initially transformed from TD to FD, and 2) the VF approach is then applied to estimate the poles and residues of the power system dominant modes with significant accuracy.

Initial results of the application of the VF to different power system configurations are presented, including conventional transmission systems, networks with distributed generation and microgrids (MG) operating in grid-connected or islanded mode. Moreover, the performance of the VF is evaluated under real-world conditions using field measurements. The accuracy of the VF is compared to other identification techniques, including Prony method, N4SID and PEM. Results verify the practical value of VF for power system mode estimation and dynamic equivalencing.

The work of T. A. Papadopoulos is supported by the 'IKY Fellowships of Excellence for Postgraduate Studies in Greece – Siemens Program'.

T. A. Papadopoulos is with the Power Systems Laboratory, Dept. of Electrical & Computer Engineering, Democritus University of Thrace, Xanthi, Greece, GR 67100, (corresponding author's e-mail: thpapad@ee.duth.gr).

T. A. Papadopoulos, A. I. Chrysochos, E. O. Kontis and G. K. Papagiannis are with the Power Systems Laboratory, School of Electrical & Computer Engineering, Aristotle University of Thessaloniki, Thessaloniki, Greece, GR 54124, (e-mail: grigoris@eng.auth.gr).

II. BACKGROUND

A. System basics

The state-space representation of a linear, time-invariant system in continuous-time form is [1]:

$$\dot{x} = \mathbf{A}_c x + \mathbf{B}_c u, \quad (1)$$

$$y = \mathbf{C}_c x + \mathbf{D}_c u, \quad (2)$$

where x is the state matrix of the system, \dot{x} denotes the derivate of x against time, u and y are the input and output variables, respectively. System matrices \mathbf{A}_c , \mathbf{B}_c , \mathbf{C}_c and \mathbf{D}_c contain the unknown system parameters. The homogeneous response of a state x_i is [1]:

$$x_i(t) = \sum_{i=1}^N A_i e^{\sigma_i t} \cos(\omega_i t + \varphi_i), \quad (3)$$

where A_i , φ_i , $\omega_i = 2\pi f_i$ and σ_i are the amplitude, angle, angular frequency and damping factor, respectively.

In discrete form (1) is rewritten as:

$$x_{k+1} = \mathbf{A}x_k + \mathbf{B}u_k, \quad (4a)$$

$$y_k = \mathbf{C}x_k + \mathbf{D}u_k, \quad (4b)$$

where all matrices are defined at the discrete time instant k . Since system matrices are determined, the eigenvalues $\lambda_i = \sigma_i \pm j\omega_i$ of \mathbf{A} or alternatively the poles of the system transfer function $H(s)$, defined in (5), can be determined. For the identification of $H(s)$ apart from pole estimation, the corresponding residues are also required.

$$H(s) = \frac{Y(s)}{U(s)} = \sum_{\ell=1}^{2N} \frac{K_\ell}{s - p_\ell}, \quad (5)$$

where p_ℓ is the pole of the transfer function related to eigenvalue λ_i of \mathbf{A} and K_ℓ is the corresponding residue.

B. Vector fitting

VF approximates a FD response with a rational function defined as the sum of $2N$ partial fractions, as shown in (6).

$$F(s) = \sum_{\ell=1}^{2N} \frac{K_\ell}{s - p_\ell} + d + s \cdot h, \quad (6)$$

where terms d and h are optional and mainly defined by the asymptotic behavior of the FD response. VF iteratively solves (6) in a least-squares (LS) sense as a two-stage linear problem. In the first stage, known as pole relocation, an initial set of poles is used to estimate iteratively the poles of (6). The improved final poles are introduced in the second stage, named as residue identification to calculate the corresponding residue values [1], [8].

Therefore, from (3), (5) and (6) it is evident that VF can be directly applied to a power system dynamic response (ringdown) to identify the mode parameters using (7).

$$A_i \cdot e^{+j\varphi_i} = 2K_\ell, \quad (7a)$$

$$A_i \cdot e^{-j\varphi_i} = 2K_{\ell+1}, \quad (7b)$$

$$\sigma_i + j\omega_i = p_\ell, \quad (7c)$$

$$\sigma_i - j\omega_i = p_{\ell+1}. \quad (7d)$$

The methodology followed in this paper to identify the dominant modes contained in a ringdown is summarized as follows:

- Transform the TD data of a ringdown to FD using the Fast Fourier Transform (FFT).
- The FD response is fitted using VF assuming relative error tolerance of -40 dB and a number of poles varying from 2 to 10.
- Identify the poles and residues of the resulting rational function. Possible artificial poles that surplus dominant modes can be easily detected and removed, since they are characterized by significantly low amplitude or high angular frequency / damping factor and/or.
- Determine the parameters of the dominant modes contained in the response using (7).

The identified mode parameters are then used to simulate the ringdown response by means of (3).

C. Model validation

The accuracy of the simulated responses obtained by VF is verified by computing the coefficient of determination R^2 and the deviation function $dev(k)$, defined in (8) and (9), respectively, for each case.

$$R^2 = \left(\frac{\sum_{k=1}^M (y(k) - \hat{y}(k))^2}{\sum_{k=1}^M (y(k) - \bar{y})^2} \right) \times 100, \quad (8)$$

$$dev(k) = \hat{y}(k) - y(k), \quad (9)$$

where \bar{y} is the mean value of the original response y and \hat{y} is the simulated response by VF and M is the total number of signal samples. The coefficient of determination is the percentage value that shows how well the simulated. The larger the R^2 is, the more accurate the fit of the simulated to the original response is, thus a 100 % value corresponds to a perfect match, while a 0 % indicates that the simulated response is a constant ($\hat{y} = \bar{y}$) [14], [15]. The identified mode parameters are evaluated using the relative prediction error (% PE):

$$\% \text{ PE} = \frac{|m_p(\text{identified}) - m_p(\text{original})|}{|m_p(\text{original})|} \cdot 100, \quad (10)$$

where m_p can any mode parameter.

III. POWER SYSTEMS UNDER STUDY

The real power dynamic responses of five test power systems (TPS) are investigated with dominant modes presented in Tables I and II. In Table I the mode damping factor and angular frequency are listed for each TPS, while in Table II the corresponding amplitude and angle are summarized. In TPS1, inter-area oscillations of a transmission system are simulated using the benchmark response provided

in [9]. In TPS2, a medium-voltage (MV) MG in grid-connected mode is considered, including two synchronous generators, two inverter-interfaced DG units and a static load. TPS3 and TPS4 correspond to a low-voltage (LV) laboratory-scale MG. The MG can operate both in grid-connected and islanded mode, and consists of the following distributed generation (DG) units: a) 2 kVA synchronous generator, b) 10 kVA inverter, c) 5 kW/3.75 kVAr static load bank, and d) 2.2 kW, 0.87 lagging asynchronous machine. All DG units follow an f - P , V - Q droop control scheme. In islanded mode an additional synchronous generator is also connected to the MG in order to provide voltage and frequency support. The dominant modes of TPS2 - TPS4 have been identified by applying Prony method on the recorded responses. Further details on TPS2 - TPS4 and on the identification procedure are provided in [10], [11]. TPS5 is the IEEE-39 bus system, also known as New-England Power System, consisting of 39 buses and 10 generators [12]. A ringdown response at bus-16 is recorded, applying a 30% load increase at bus-21. Originally, the dominant modes contained in the ringdown are identified by applying offline PEM to simulated responses.

TABLE I
DOMINANT MODES OF THE TEST SYSTEMS

Test Power System	Mode #1		Mode #2		Mode #3	
	σ_1 (1/s)	f_1 (Hz)	σ_2 (1/s)	f_2 (Hz)	σ_3 (1/s)	f_3 (Hz)
TPS1	-0.11	0.25	-0.16	0.39	-	-
TPS2	-4.17	4.29	-11.8	7.73	-	-
TPS3	-2.60	3.31	-	-	-	-
TPS4	-0.89	0.21	-39.0	2.78	-	-
TPS5	-0.17	0.23	-0.81	0.63	-1.82	1.03

TABLE II
MODE AMPLITUDE AND ANGLE OF THE TEST SYSTEMS

Test Power System	Mode #1		Mode #2		Mode #3	
	A_1 (pu)	φ_1 (rad)	A_2 (pu)	φ_2 (rad)	A_3 (pu)	φ_3 (rad)
TPS1	2.00	1.5π	2.0	0.5π	-	-
TPS2	2.09	0.35π	1.5	-1.26π	-	-
TPS3	1.00	1.5π	-	-	-	-
TPS4	2.59	-0.55π	10.0	-0.59π	-	-
TPS5	1.00	-0.8π	1.32	-0.6π	1.13	0.09π

IV. NUMERICAL RESULTS

A. Regular vs odd sampling

The application of VF for mode identification is evaluated for TPS1 using MATLAB implementation. The examined dynamic response is described by (11) and simulates a ringdown obtained by a phasor measurement unit (PMU). The testing data are generated at sampling rate of $1/T_s = 1000$ samples per second (sps), assuming total observation time T equal to 30 s and 60 s.

$$y_{TPS_1}(t) = 2e^{-0.11t} \cos(2\pi \cdot 0.25 \cdot t + 1.5\pi) + 2e^{-0.16t} \cos(2\pi \cdot 0.39 \cdot t + 0.5\pi). \quad (11)$$

The spectrum of the dynamic responses is calculated using

both regular and odd sampling schemes in FD [13], defined in (12) and (13), respectively.

$$F_k = T_s \cdot \sum_{n=0}^{N_w-1} f_n \cdot e^{-j2\pi kn/N_w}, k=0,1,\dots,N_w-1 \quad (12)$$

$$F_{2k+1} = T_s \cdot \sum_{n=0}^{N_w-1} f_n \cdot e^{-j2\pi kn/N_w} \cdot e^{-j\pi n/N_w}, k=0,1,\dots,N_w-1 \quad (13)$$

where

$$f_n = f(n \cdot T_s) \quad (14)$$

and N_w is the total number of the generated samples. Both sampling schemes assume equally spaced samples. However, in the regular sampling case the frequency spacing is equal to $\Delta\omega$, while in the odd sampling is $2\Delta\omega$, where $\Delta\omega = \pi/T$. The two sampling methods are compared for different observation times in Figs. 1 and 2, where the spectrum magnitude and angle are plotted, respectively.

The two peaks in Fig. 1 are directly associated with the frequencies of the two ringdown modes. As depicted in Fig. 1 the corresponding frequencies of the two peaks for both sampling schemes are closer to the original values when T is 60 s rather than 30 s, due to the higher frequency discretization. Small differences in the spectrum magnitude and angle between the two methods are mainly noticed in the frequency range close to the spectrum peaks.

The spectrum of the ringdown calculated with regular and odd sampling is fitted with VF. In all cases the resulting model order corresponds to two pairs of conjugate poles, neglecting any surplus modes as previously analyzed. In Fig. 3 and Fig. 4 the magnitude and angle deviation between the fitted and the original spectrum is illustrated, respectively. It can be seen that negligible differences are observed in the case of the regular sampled spectrum, while significant deviations occur in the case of odd sampling, especially for $T = 30$ s.

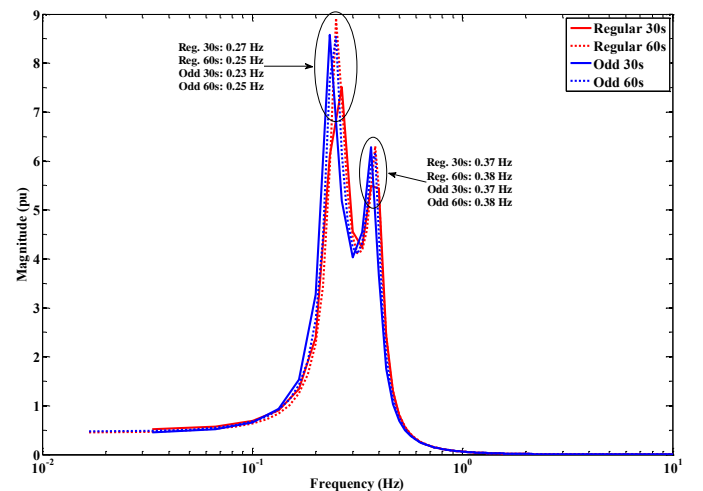


Fig. 1. Spectrum magnitude comparison with regular and odd sampling.

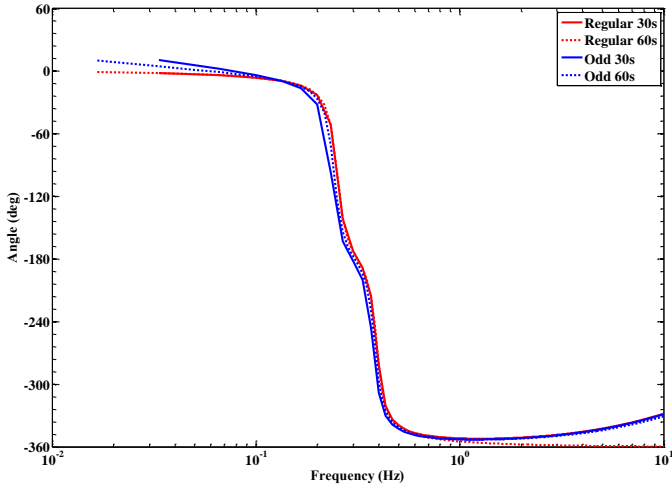


Fig. 2. Spectrum angle comparison with regular and odd sampling.

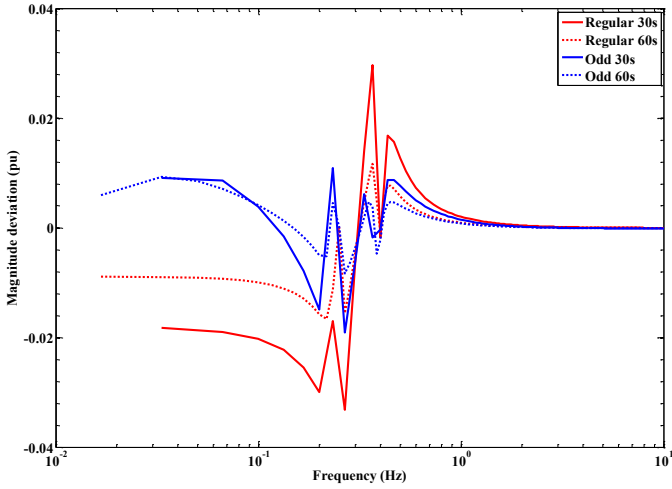


Fig. 3. Magnitude deviation between fitted and original spectrum.

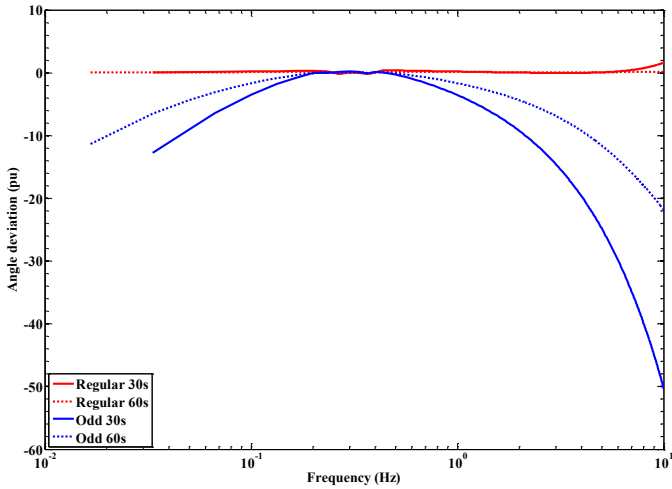


Fig. 4. Angle deviation between fitted and original spectrum.

The resulting TD responses are compared to the original response of Fig. 5 by plotting in Fig. 6 the corresponding deviation curves. In the case of regular sampling the simulation error is very low for both observation times, where $dev(k)$ is lower than $1E-3$ and R^2 is in average 99.96 %. On the contrary, the simulated response using odd sampling

presents significant errors, especially for the case of $T = 30$ s, since a considerable phase shift in the TD response is introduced. This is mainly attributed to the fact that for a given observation time and number of samples the frequency range of the odd sampling is double compared to regular. This results in low frequency resolution in the low-frequency range where the frequencies of the contained oscillatory modes are located.

From the above analysis it is observed that the efficiency of VF with regular sampling is significantly high and superior to odd sampling in all examined cases. More specifically, the % PE of the identified mode parameters to the original values are presented in Table III for the case of $T = 30$ s, assuming FD regular sampling. The efficiency of the proposed procedure for mode identification is verified, since the estimates of all mode parameters are consistent.

The accuracy of the proposed methodology is also evaluated for all other TPSs. In Table IV the R^2 of the simulated ringdown responses is presented, assuming TD sampling rate 1000 sps and FD regular sampling. It can be noticed that significantly high R^2 values are obtained, exceeding 99 % in all cases. Note that the observation time of each ringdown is also presented in Table IV.

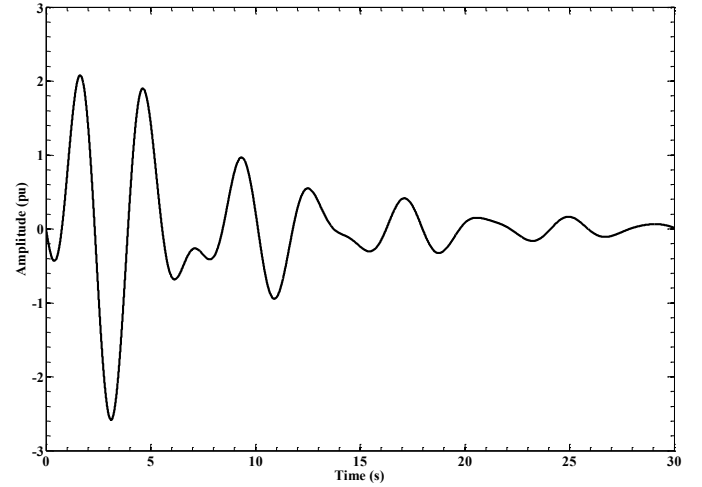


Fig. 5. Original ringdown response.

TABLE III
% PE OF THE IDENTIFIED MODAL PARAMETERS

Mode Parameter	Mode #1	Mode #2
σ	0.7260	0.5625
ω	0.0507	0.0548
A	0.3100	0.3710
φ	0.3947	0.9040

TABLE IV
COEFFICIENT OF DETERMINATION FOR DIFFERENT TEST POWER SYSTEMS

Test System	R^2	Observation time (s)
TPS1	99.9204	30
TPS2	99.9778	2
TPS3	99.9933	2
TPS4	99.7817	3
TPS5	99.9958	30

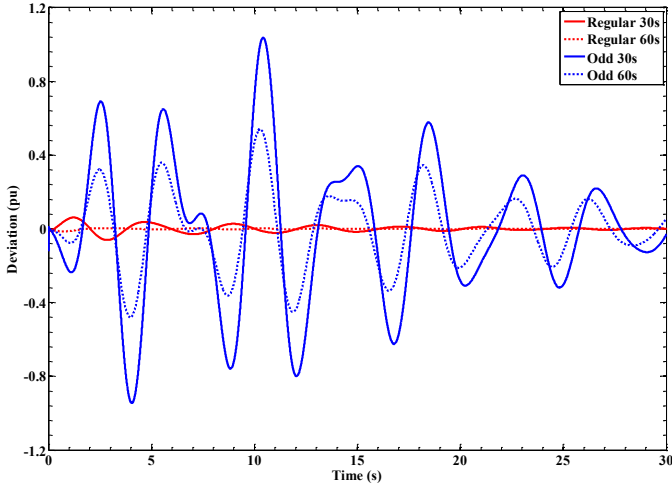


Fig. 6. Comparison of TD responses with deviation curves.

B. Effect of sampling rate

In this section the influence of the sampling rate on mode estimation is investigated. VF is applied to identify the modes of all TPSs with different sampling rates. The R^2 curve of the simulated dynamic responses is plotted against sps in Fig. 7. Note that x axis is in logarithmic scale. In general, significant increase of R^2 is observed with the sampling rate. Specifically, R^2 is close to 97 % for sps equal to 100, while further increase of the sps improves slightly the simulated responses.

Specifically, in Fig. 8 the % PE curve of the identified mode parameters for TPS 5 is plotted. Note that both axes are in logarithmic scale. It can also be observed that the % PE decreases with increasing sampling rate for both damping factors and angular frequency of the three modes. The % PE of all mode parameters is lower than 0.02 % for sampling rates higher than 100. Furthermore, the lower frequency modes are estimated more accurately than the higher frequency modes. The same investigation is also applied to the rest TPSs and the results are summarized in Table V for sps 1000. Note that the % PE of all mode parameters is significantly low, with the exception of mode # 2 in TPS4, where the damping factor is very high.

Moreover, the performance of VF considering the computational burden is investigated in an Intel Core i7, 2.67 GHz, RAM 6 GB personal computer. The processing time in seconds is presented in Table VI for all examined TPSs and for different sampling rates taking values from 10 sps to 10000 sps. It is evident that VF can extract the dominant modes very fast even in cases of high sampling rates up to 1000 sps, allowing the online application of the procedure. Note that computational time of the order of seconds is only noticed in cases of large PMU data streams and excessive sampling rates, i.e. for 10000 sps.

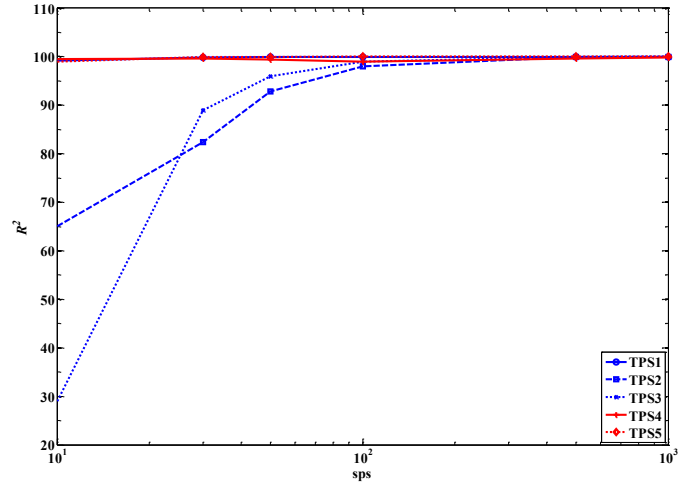


Fig. 7. Effect of sps for different TPS configurations.

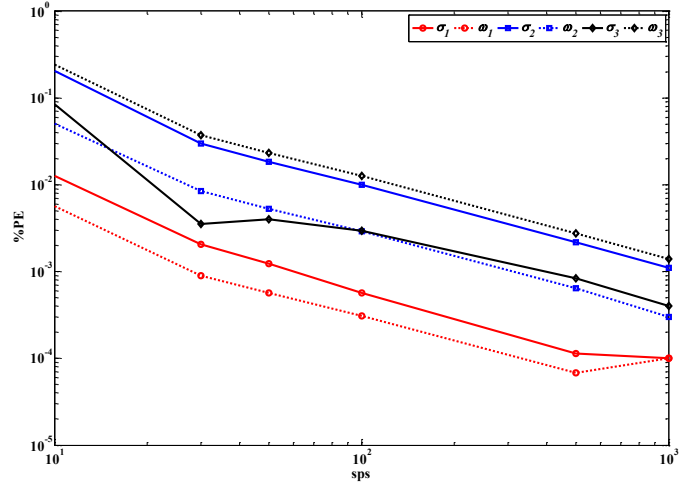


Fig. 8. Mode parameter % PE for TPS5.

TABLE V
% PE IN MODE ESTIMATION FOR 1000 SPS

Test System	Mode #1		Mode #2		Mode #3	
	σ_1	f_1	σ_2	f_2	σ_3	f_3
TPS1	0.0464	0.0047	0.0578	0.0044	-	-
TPS2	0.0080	0.0024	0.0371	0.0145	-	-
TPS3	0.0005	0.0002	-	-	-	-
TPS4	0.1080	0.0333	2.7050	9.7051	-	-
TPS5	0.0001	0.0001	0.0011	0.0003	0.0004	0.0014

TABLE VI
COMPUTATIONAL BURDEN IN SECONDS

Test System	sps					
	10	50	100	500	1000	10000
TPS1	0.0256	0.0548	0.0940	0.4321	0.7761	8.504
TPS2	0.0182	0.0218	0.0260	0.0623	0.1082	0.912
TPS3	0.0126	0.0141	0.0159	0.0279	0.1564	0.343
TPS4	0.0215	0.0311	0.0439	0.1564	0.3305	3.169
TPS5	0.0377	0.1071	0.1946	0.8154	1.623	17.89

C. Identification of frequency close modes

In this test the performance of VF is evaluated in case frequency close modes are contained in the ringdown. Considering the ringdown response of TPS5, the mode #3 is manually replaced by a mode at 0.66 Hz with damping factor

equal to the original. The resulting ringdown contains two close modes at 0.63 Hz and 0.66 Hz, i.e. modes #2 and #3. The TD response is generated using 1000 sps, while the FD is regularly sampled. The spectrum of the generated dynamic response is fitted with VF, as shown in Fig. 9 and Fig. 10. The spectrum contains only two peaks instead of the expected three, since close modes #2 and #3 cannot be resolved with conventional Fourier techniques. However, VF preserves its high precision and identifies all three modes as analyzed in Table VII. This feature of VF to identify frequency close modes is an advantage compared to other FD system identification techniques. In Fig. 11 the simulated TD system response is plotted and compared to the original, presenting in average trivial deviation. Note that the maximum deviation is $5.6E-3$. Also note that the dynamic responses axis is depicted on the left of the graph, while the deviation curve refers to the right one.

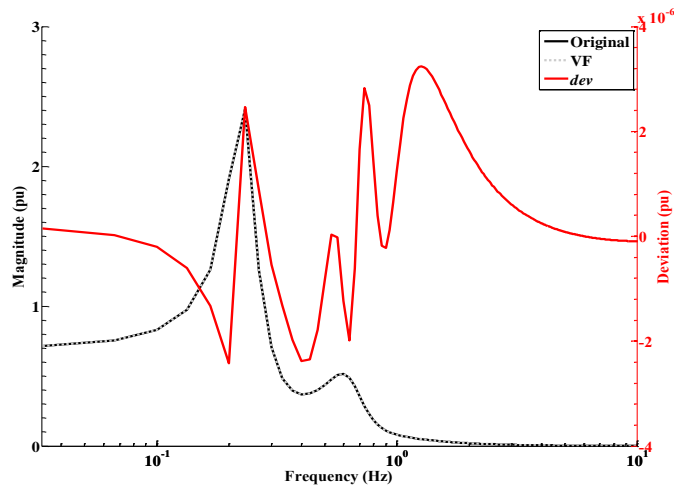


Fig. 9. Spectrum magnitude fitting of the modified TPS5 with close modes.

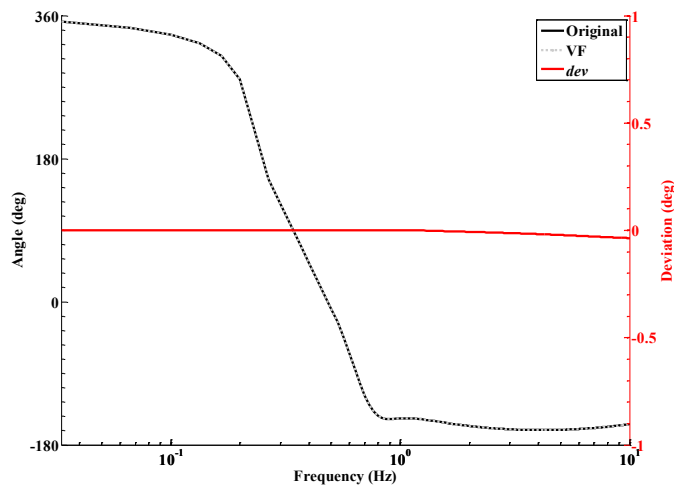


Fig. 10. Spectrum angle fitting of the modified TPS5 with close modes.

TABLE VII
% PE OF THE IDENTIFIED MODAL PARAMETERS

Parameter	Mode #1	Mode #2	Mode #3
σ	1.26E-4	4.1E-3	1.2E-3
ω	3.3E-5	1.2E-3	9.9E-3
A	3.7E-1	1.3E-2	1.9E-2
φ	2.0E-1	1.1E-2	6.4E-2

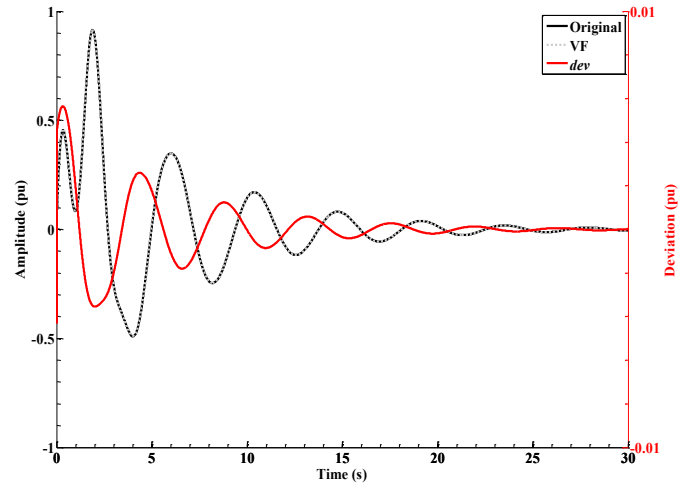


Fig. 11. Comparison of the original and the fitted TD response.

V. APPLICATION TO FIELD MEASUREMENTS

VF is applied to the real measurement dataset obtained from TPS3 for mode identification. In this analysis the MG is interconnected to a weak distribution system. The MG real and reactive power responses at the point of common coupling (PCC) are recorded with a sample rate of 500 sps. The disturbances are caused by rapid changes in the operational state of the static load [10].

Since measurement data are distorted by noise, preprocessing is performed prior to parameter estimation to focus on the low-frequency modes and improve the quality of the measured data. The discretized real and reactive power responses are passed through 100-order finite impulse response (FIR) zero-phase low pass filters (LPF) with cut-off frequency at 3 Hz and 50 Hz, respectively [5], [14], [16]. The processing of the recorded responses is implemented in MATLAB using the available Digital Signal Processing (DSP) toolbox [15].

By applying VF the single mode contained in the real power response referred in Section III is identified. Additionally, the reactive power is described by two modes. In Figs. 12 and 13 the TD simulated real and reactive power responses, respectively, are compared to the corresponding measurements. Both real and reactive power deviation curves indicate the high accuracy of the fitted responses. Note that deviation curves are calculated assuming in $y(k)$ of (9) the measurement responses after filtering.

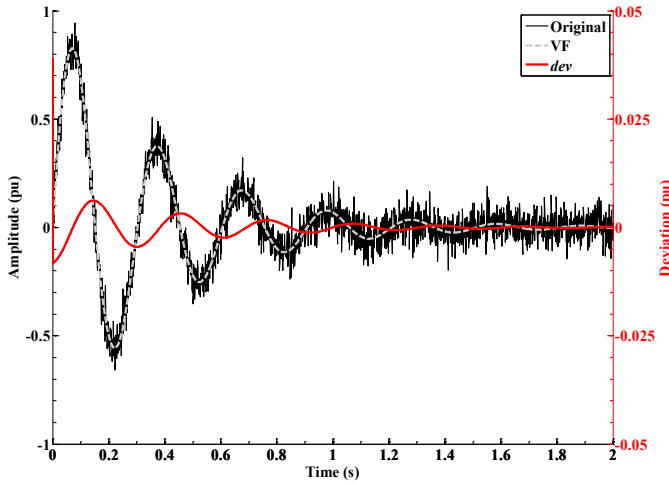


Fig. 12. Comparison of the original and the fitted TD real power response.

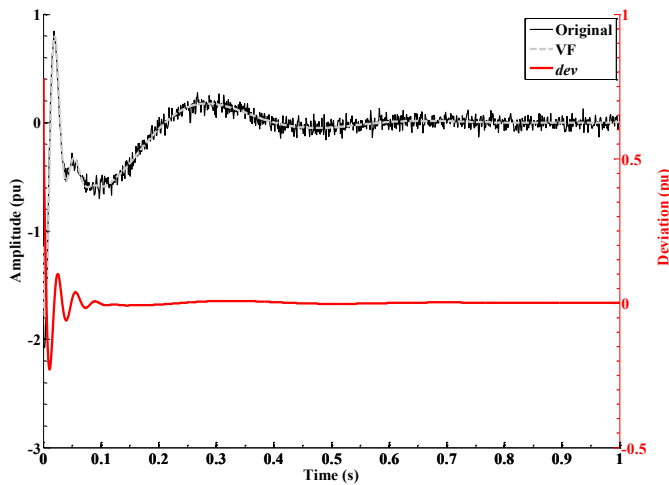


Fig. 13. Comparison of the original and the fitted TD reactive power response.

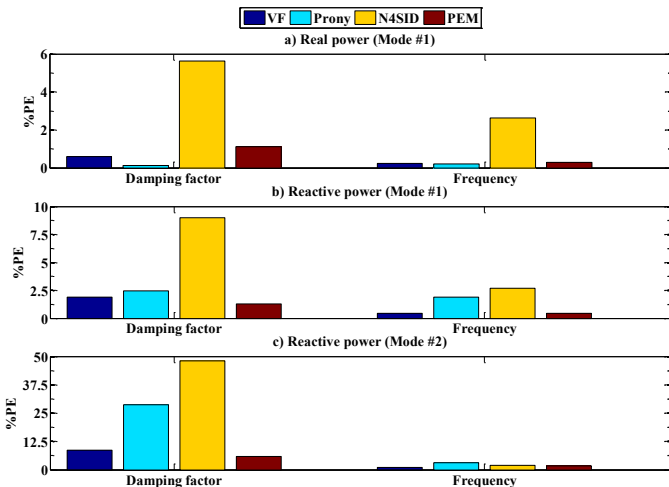


Fig. 14. % PE in mode parameter estimation. Subplots: a) mode #1 real power, b) mode #1 reactive power and c) mode #2 reactive power.

The performance of VF is assessed and compared with Prony, N4SID and PEM techniques in Fig. 14, where the bar diagrams illustrate the % PE of the identified modes for each case. It can be seen that the performance of VF is comparable to PEM in terms of accuracy for both the damping factor and

the angular frequency. The % PE is lower than 10 % for all mode parameters for the two methods. Considering N4SID, it has the worst performance and the highest % PE in the damping estimate of the modes #1 and #2 of the reactive power with 8.99 % and 48.1 % error, respectively. Prony method generally provides accurate results in terms of parameter mode estimation. However, the resulting damping factor of mode #2 of the reactive power presents a 28.7 % error.

VI. CONCLUSIONS

In this paper VF has been employed for transfer function identification and mode estimation of power systems, based on recorded dynamic responses. A parameter estimation procedure is proposed and the influence of different model parameters is investigated. The main remarks indicate that:

- VF can very accurately approximate the FD response of ringdowns in power systems, and thus identify the corresponding mode parameters with high accuracy.
- For the calculation of the ringdown spectrum, regular sampling is preferred over the odd sampling method.
- The application of up-sampling in TD can improve significantly mode estimation with VF.
- A significant feature of VF is its capability to accurately identify closely spaced modes.
- VF can be efficiently applied both to offline simulated responses and also to measured data, distorted by high-frequency noise or harmonics. For the latter case the application of LPFs improves significantly mode estimation.
- Comparing VF with other well-known system identification techniques it is concluded that the performance of VF is high and comparable to PEM in terms of accuracy for both damping and frequency estimates.
- VF can be efficiently applied for real-time dynamic response monitoring.

VII. REFERENCES

- [1] IEEE Task Force on Identification of Electromechanical modes, "Identification of electromechanical modes in power systems," IEEE Power & Energy Society, Tech. Rep. PES-TR15, Jun. 2012. [Online]. Available: <http://resourcecenter.ieee-pes.org/>.
- [2] J.R. Smith, F. Fatehi, C.S. Woods, J.F. Hauer, and D. J. Trudnowski, "Transfer function identification in power system applications," *IEEE Trans. Power Syst.*, vol. 8, no. 3, pp. 1282-1290, 1993.
- [3] J. F. Hauer, C.J. Demeure, and L.L. Sharf, "Initial results in Prony analysis of power system response signals," *IEEE Trans. Power Syst.*, vol. 5, no. 1, pp. 80-89, 1990.
- [4] T. Katayama, *Subspace Methods for System Identification*, London: Springer, 2005, p. 8-11.
- [5] L. Ljung. (2013, Sep.), *System Identification Toolbox: User's Guide*. The Mathworks Inc., Natick, MA. [Online]. Available: www.mathworks.com/help/pdf_doc/ident/ident.pdf
- [6] Z. Tashman and H. Khalilinia, V. Venkatasubramanian, "Multi-dimensional Fourier ringdown analysis for power systems using synchrophasors," *IEEE Trans. Power Syst.*, vol. 29, no. 2, pp. 731-741, 2014.

- [7] B. Gustavsen and A. Semlyen, "Rational approximation of frequency domain responses by vector fitting," *IEEE Trans. Power Del.*, vol. 14, no. 3, pp. 1052-1061, 1999.
- [8] B. Gustavsen, "Improving the pole relocating properties of vector fitting," *IEEE Trans. Power Del.*, vol. 21, no. 3, pp. 1587-1592, 2006.
- [9] N. Zhou, J. Pierre, and D. Trudnowski, "A Stepwise Regression Method for Estimating Dominant Electromechanical Modes," *IEEE Trans. Power Systems*, vol. 27, no.2, pp.1051-1059, May 2012.
- [10] P.N. Papadopoulos, T.A. Papadopoulos, P. Crolla, A.J. Roscoe, G.K. Papagiannis, and G.M. Burt, "Black-box dynamic equivalent model for microgrids using measurement data," *IET Gener., Trans. & Distrib.*, vol. 7, no. 1, pp. 1-11, 2013.
- [11] P. N. Papadopoulos, T.A. Papadopoulos, P. Crolla, A.J. Roscoe, G.K. Papagiannis, G.M. Burt, "Measurement-based Analysis of the Dynamic Performance of Microgrids using System Identification Techniques," *IET Gener., Trans. & Distrib.*, vol.9, no.1, pp.90-103, 2015.
- [12] M. A. Pai, *Energy function analysis for Power System stability*, Kluwer Academic Publishers, 1989.
- [13] P. Moreno and A. Ramirez, "Implementation of the numerical Laplace transform: A review task force on frequency domain methods for EMT studies," *IEEE Trans. Power Del.*, vol. 23, no. 4, pp. 2599-2609, 2008.
- [14] J.V. Milanovic, S. Mat Zali, "Validation of Equivalent Dynamic Model of Active Distribution Network Cell," *IEEE Trans. on Power Systems*, vol.28, no.3, pp.2101-2110, 2013
- [15] Matlab R2011b, Available at <http://www.mathworks.com>.
- [16] Z. Ning, J. W. Pierre, J. F. Hauer, "Initial results in power system identification from injected probing signals using a subspace method," *IEEE Trans. Power Syst.*, vol. 21, no. 3, pp. 1296-1302, 2006.